BIOCHEMISTRY
including biophysical chemistry & molecular biology
Article

*Biochemistry* **2011,** *50,* 945–952 945
DOI: 10.1021/bi101597k

# C-Terminal Tyrosine Residues Modulate the Fusion Activity of the Hendra Virus Fusion Protein†

Andreea Popa, Cara Teresia Pager, and Rebecca Ellis Dutch*

*Department of Molecular and Cellular Biochemistry, University of Kentucky, Lexington, Kentucky 40536, United States*

*Received October 1, 2010; Revised Manuscript Received December 17, 2010*

ABSTRACT: The paramyxovirus family includes important human pathogens such as measles, mumps, respiratory syncytial virus, and the recently emerged, highly pathogenic Hendra and Nipah viruses. The viral fusion (F) protein plays critical roles in infection, promoting both the virus−cell membrane fusion events needed for viral entry as well as cell−cell fusion events leading to syncytia formation. We describe the surprising finding that addition of the short epitope HA tag to the cytoplasmic tail (CT) of the Hendra virus F protein leads to a significant increase in the extent of cell−cell membrane fusion. This increase was not due to alterations in surface expression, cleavage state, or association with lipid microdomains. Addition of a Myc tag of similar length did not alter Hendra F protein fusion activity, indicating that the observed stimulation was not solely a result of lengthening the CT. Three tyrosine residues within the HA tag were critical for the increase in the extent of fusion, suggesting C-terminal tyrosines may modulate Hendra fusion activity. The effects of addition of the HA tag varied with other fusion proteins, as parainfluenza virus 5 F-HA showed a decreased level of surface expression and no stimulation of fusion. These results indicate that additions to the C-terminal end of the F protein CT can modulate protein function in a sequence specific manner, reinforcing the need for careful analysis of epitope-tagged glycoproteins. In addition, our results implicate C-terminal tyrosine residues in the modulation of the membrane fusion reaction promoted by these viral glycoproteins.

Paramyxoviruses are enveloped, negative-stranded RNA viruses that enter cells by fusion with a cellular membrane (*1*). Membrane fusion is promoted by specific viral glycoproteins, which mediate both attachment of the virus to target cells and subsequent fusion of the viral and cellular lipid bilayers. Most paramyxoviruses require both an attachment (HN, H, or G) and a fusion (F)[1] protein to enter cells, with fusion generally occurring at neutral pH (*1*, *2*). The Hendra and Nipah viruses are recently emerged, highly pathogenic zoonotic paramyxoviruses, classified as biosafety level four pathogens because of their ability to infect humans, high mortality rates, the absence of treatments or vaccines, and the possibility of human to human transmission (*3*). The attachment (G) and fusion (F) proteins are both required for Hendra and Nipah membrane fusion and viral entry. Hendra F is a 546-amino acid type I integral membrane protein, which folds as a homotrimer and is post-translationally modified by the addition of carbohydrate chains (*4*). Similar to other class I fusion proteins, Hendra F contains a fusion peptide (FP), two heptad repeat regions (HRA and HRB), a transmembrane domain (TM), and a 28-amino acid cytoplasmic tail (CT) (Figure 1).

Paramyxovirus F proteins require proteolytic processing of the $F_0$ inactive precursor to the fusogenically active $F_1+F_2$ form. This cleavage event positions the fusion peptide at the N-terminus of the newly formed $F_1$ subunit. While the majority of paramyxovirus F proteins are cleaved by furin within the trans-Golgi network (*5*−*8*), processing of Hendra and Nipah F requires endocytic recycling (*9*−*13*) and cleavage by the endosomal/lysosomal protease cathepsin L (*10*, *11*). A YXXΦ endocytosis motif within the F CT (where X represents any amino acid and Φ a hydrophobic amino acid) is critical for Hendra and Nipah F endocytosis and cathepin L proteolytic processing (*9*−*13*).

Following cathepsin L cleavage, Hendra and Nipah F are recycled to the cell surface, where they are thought to interact with the attachment protein, G (*10*, *14*, *15*). G binding to the cellular receptors ephrin B2 and/or B3 (*16*, *17*) is hypothesized to disrupt the F−G interaction, leading to triggering of membrane fusion by F (*15*, *18*−*20*). Mutations that inhibit the F−G interaction also inhibit membrane fusion (*18*), and the avidity of the F−G interaction is inversely proportional to fusion activity (*19*, *20*). Once F is triggered, the FP inserts into the target membrane and the HRB and HRA domains form a six-helix bundle complex, which is hypothesized to provide the energy necessary for membrane merger (*21*). The crystal structures of the prefusion form of PIV5 F (*22*) and of the postfusion forms of Newcastle disease virus (NDV) and human parainfluenza virus 3 (HPIV3) F (*23*−*25*) have been determined, greatly contributing to the understanding of the refolding events that take place in the ectodomain of paramyxovirus fusion proteins. However, the crystal structures lack the membrane-interacting TM domain and the CT of F, two regions that have also been shown to play important roles in the fusion process (*2*, *26*, *27*).

†This work was supported by NIAID/NIH grant R01AI051517, NIH grant #U54 AI057157 from the Southeastern Regional Center of Excellence for Emerging Infections and Biodefense and NIH Grant Number 2P20 RR020171 from the National Center for Research Resources.

*To whom correspondence should be addressed: Department of Molecular and Cellular Biochemistry, University of Kentucky College of Medicine, B171 BBSRB, 741 S. Limestone, Lexington, KY 40536-0509. Phone: (859) 323-1795. Fax: (859) 323-1037. E-mail: rdutc2@uky.edu.

[1]Abbreviations: PIV5, parainfluenza virus 5; F, fusion; CT, cytoplasmic tail; TM, transmembrane domain; HRA and HRB, heptad repeats A and B, respectively; NDV, Newcastle disease virus; HPIV 2 and 3, human parainfluenza viruses 2 and 3, respectively.


Published on Web 12/23/2010

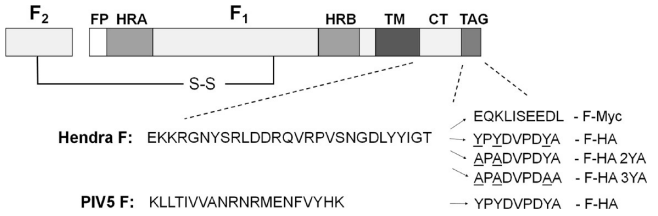


FIGURE 1: Schematic representation of the Hendra virus fusion protein. Abbreviations: FP, fusion peptide; HR, heptad repeat; TM, transmembrane domain; CT, cytoplasmic tail. The sequences of Hendra F or the PIV5 F cytoplasmic tail, as well as the sequences of the Myc and HA epitope tags, are presented. F-HA 2YA and 3YA contain tyrosine to alanine substitutions in the HA tag.

To aid in our investigation of the function and intracellular trafficking of Hendra F and G, we added a HA epitope tag (YPYDVPDYA) to the CT of Hendra F and Hendra G, as no monoclonal antibodies were available. Surprisingly, addition of the HA tag to Hendra F significantly increased membrane fusion activity. To examine if extension of the Hendra F CT stimulates fusion activity in a sequence-independent manner, we added a Myc epitope tag (EQKLISEEDL). No increase in the level of fusion was observed, suggesting a sequence specific effect of the HA tag. Further mutational analysis demonstrated that the three tyrosine residues present in the HA tag are critical for the observed fusion stimulation. Finally, to determine if HA tag-stimulated fusion is a general effect, we added the HA tag to the CT of parainfluenza virus 5 (PIV5) F protein. Fusion stimulation was not observed, and the overall level of protein expression was significantly reduced. These results indicate that the C-terminal end of the Hendra F CT modulates fusion in a sequence specific manner, with tyrosine residues in this region specifically enhancing membrane fusion activity.

## EXPERIMENTAL PROCEDURES

*Cell Lines*. Vero, baby hamster kidney (BHK), and BSR cells (kindly provided by K.-K. Conzelman, Pettenkofer Institut, Munich, Germany) were maintained in Dulbecco's modified Eagle's medium (DMEM, Gibco Invitrogen) supplemented with 10% fetal bovine serum (FBS) and 1% penicillin-streptomycin.

*Plasmids*. Hendra F and G genes were kindly provided by L. Wang (Australian Animal Health Laboratory, Geelong, Australia) and were subcloned into the pCAGGS mammalian expression vector as previously described (*28*). pCAGGS-PIV5 F and HN were kindly provided by R. Lamb (Howard Hughes Medical Institute, Northwestern University, Evanston, IL). Primers designed to add the HA or Myc tags were utilized in polymerase chain reactions (PCRs) performed using pGEM-Hendra F or G and pGEM-PIV5 F or HN as a template. The PCR products were ligated into pCR-Blunt TOPO (Invitrogen), sequenced, and subcloned into EcoRI-digested pCAGGS. The constructs were sequenced in their entirety.

*Antibodies*. Polyclonal antibodies (Genemed Custom Peptide Antibody Service, San Francisco, CA) were generated to residues 526−539 or 516−529 of Hendra F or PIV5 F CT, respectively, and to residues 19−33 of the Hendra G CT (Genemed Synthesis, Inc., San Francisco, CA).

*Expression of HeV and PIV5 Fusion and Attachment Proteins*. The wild-type or the tagged proteins were expressed in subconfluent monolayers of Vero cells using the pCAGGS expression system and Lipofectamine Plus (Life Technologies, Carlsbad, CA) according to the manufacturer's protocol. After 3−4 h at 37 °C, the transfection medium was replaced with DMEM supplemented with 10% FBS and 1% penicillin-streptomycin.

*Pulse−Chase Biotinylation Experiments*. Twenty hours post-transfection, cells were metabolically labeled with Tran $^{35}$S (100 $\mu$Ci/mL; MP Biomedicals) for 2 h. Following labeling, cells were washed twice with PBS$^-$ and chased (DMEM, 10% FBS, and 1% penicillin-streptomycin) for 4, 8, and 22 h. The samples for the 0 h time point were washed three times with ice-cold PBS at pH 8, and cells were then biotinylated using 1 mL of EZ-Link sulfo-*N*-hydroxysuccinimide-biotin (sulfo-NHS-biotin, 1 mg/mL; Pierce, Rockford, IL) in PBS$^-$ (pH 8) by being rocked gently for 30 min at 4 °C (*9*, *29*, *30*). Cells were then washed three times in ice-cold PBS$^-$ (pH 8) and lysed in RIPA lysis buffer supplemented with protease inhibitors and 25 mM iodoacetamide (*9*). At the end of each chase interval, the surface proteins were similarly biotinylated. Lysates were cleared, and immunoprecipitation with Hendra F antipeptide antibodies and protein A-conjugated Sepharose beads and separation of biotinylated proteins using streptavidin beads were performed as described previously (*29*, *30*). The total and surface fractions of the proteins were analyzed on 15% sodium dodecyl sulfate−polyacrylamide gel electrophoresis (SDS−PAGE) gels under reducing conditions and visualized using the Typhoon imaging system (GE Healthcare, Piscataway, NJ).

*Analysis of Surface Expression following Overnight Labeling*. Six to nine hours following transfection of Vero cells with wild-type or tagged forms of Hendra or PIV5 F, Vero cells were radiolabeled for 15 h using 2 mL of overnight labeling medium (89% cysteine- and methionine-deficient DMEM, 5% normal DMEM, 5% FBS, and 1% penicilin-streptomycin), to which Tran $^{35}$S was added (100 $\mu$Ci/mL). The cells were washed three times with ice-cold PBS$^-$ (pH 8), followed by biotinylation, immunoprecipitation, and streptavidin pull downs as described above. The proteins were analyzed on 15% SDS−PAGE gels and visualized using the Typhoon imaging system.

*Syncytia Assay*. Subconfluent monolayers of Vero cells were transfected with wild-type Hendra F, PIV5 F, or the described epitope-tagged constructs, in the presence or absence of the respective attachment protein. The F:G ratio was 1:2 (0.5 $\mu$g of F and 1 $\mu$g of G), and the transfection was performed using Lipofectamine Plus. The plates were incubated at 37 °C, and 24 h post-transfection, cells were washed twice with PBS$^-$ and 2 mL of DMEM (10% FBS and 1% penicillin-streptomycin) was added. Syncytia formation was examined 24−48 h post-transfection using a Nikon TS 100 inverted phase contrast microscope, and cells were photographed 48 h post-transfection at 100× magnification using a Nikon Coolpix 995 digital camera. Syncytia formation was also examined at 32 °C. Transfection was performed as described above, with cells being initially incubated at 37 °C for 18 h and then transferred to 32 °C. Seventy-two hours post-transfection, the cells were photographed.

*Luciferase Reporter Gene Assay*. Subconfluent monolayers of Vero cells in six-well plates were transiently cotransfected with wild-type or tagged Hendra F and G (or PIV5 F and HN) at 1:2 ratios (0.5 $\mu$g of F and 1 $\mu$g of G or HN), and the T7 plasmid containing the luciferase gene under the control of the T7 promoter (0.8 $\mu$g). Twenty hours post-transfection, BSR cells, which constitutively express T7 polymerase, were overlaid on the transfected Vero cells for 3 h, at ~1:1 ratios. Luciferase activity was examined using a luciferase assay system (Promega), according to the manufacturer's protocol. Light emission was quantified using an Lmax luminometer (Molecular Devices, Sunnyvale, CA).

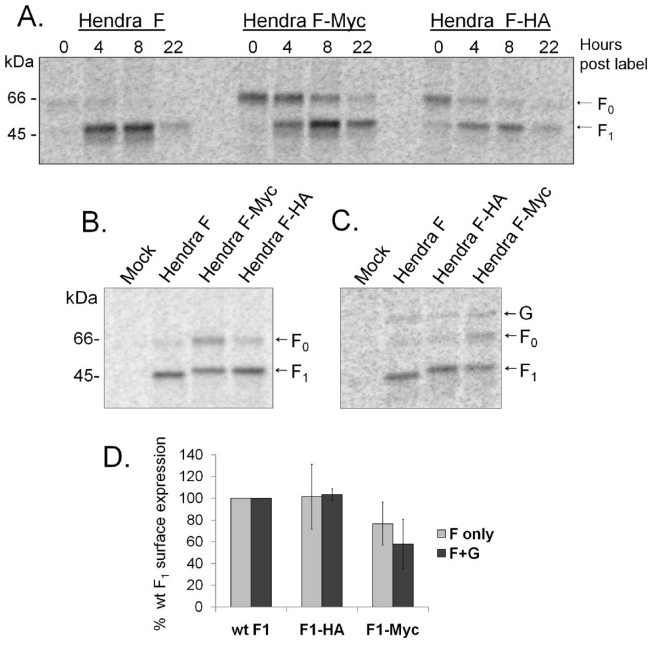


FIGURE 2: Surface expression of the wild-type and tagged Hendra F proteins. (A) Pulse−chase and cell surface biotinylation. Vero cells expressing wild-type or tagged Hendra F proteins were metabolically labeled for 2 h and chased for 0, 4, 8, and 22 h. At the end of each chase interval, surface proteins were labeled with biotin. Proteins were immunoprecipitated, and the surface population was then separated using streptavidin agarose beads, resolved on a 15% polyacrylamide gel, and visualized using the Typhoon imaging system. (B and C) Hendra F, F-Myc, and F-HA surface expression after an overnight label, in the absence (B) or presence (C) of the Hendra G protein. The surface proteins were biotinylated and visualized as described above. (D) Quantitation of Hendra F, F-HA, and F-Myc surface expression using ImageQuant version 5.2. Expression of F (in the absence of G) represents results from four independent experiments, and the error bars represent the 95% confidence interval. Expression of F in the presence G represents results from two independent experiments, and the error bars represent the 95% confidence interval.

## RESULTS

*C-Terminal Addition of HA and Myc Tags Does Not Alter Hendra F Expression or Overall Processing*. A nine-amino acid HA epitope tag (YPYDVPDYA) or a ten-amino acid Myc tag (EQKLISEEDL) was added to the C-terminus of the Hendra virus F protein (Figure 1). To determine if these additions affected protein expression or proteolytic cleavage, the tagged Hendra F proteins were transiently expressed in Vero cells using the pCAGGS system (*28*, *31*) and examined by pulse−chase analysis combined with surface biotinylation. The cells were metabolically labeled for 2 h and chased for 0, 4, 8, and 22 h, followed by biotinylation of the surface proteins. The surface Hendra F population was isolated by immunoprecipitation, followed by streptavidin pull down. Proteins were separated by SDS−PAGE and visualized by storage phosphor autoradiography (Figure 2A). Little wild-type Hendra F protein was on the surface at 0 h, consistent with previous results (*9*) suggesting that most of the protein had entered the recycling pathway utilized for proteolytic processing at this time. By 4 h, the majority of both the wild-type F and Hendra F-HA was cleaved and recycled to the cell surface, indicating similar kinetics of cathepsin L processing. In contrast, Hendra F-Myc was proteolytically processed more slowly, with a greater fraction than wild-type F present on the cell surface in the $F_0$ uncleaved form at all time points examined (Figure 2A).

The steady-state surface density of the tagged forms of Hendra F was examined by cell surface biotinylation following an overnight metabolic label. Surface expression was analyzed when F was expressed alone (Figure 2B), or together with the attachment protein G (Figure 2C), and the surface density of the fusogenically active $F_1$ form was quantified from four independent experiments (Figure 2D). In both cases, Hendra $F_1$-HA was present on the cell surface at levels similar to that of wild-type $F_1$, while Hendra $F_1$-Myc was expressed at approximately 60−75% (Figure 2D). The slowed processing of F-Myc compared to wild-type Hendra F or F-HA resulted in approximately 35% of Hendra F-Myc being present on the cell surface in the uncleaved $F_0$ form following a 15 h label, while only 8% of wild-type Hendra F was still present on the cell surface in the uncleaved form. These results suggest that specific residues in Hendra F-Myc CT modulate Hendra F processing and/or recycling.

*Addition of the HA Tag to Hendra F Significantly Enhances Syncytia Formation*. To examine the effect of short tags on the fusion activity of Hendra F, syncytia formation was assessed in Vero cells transiently expressing wild-type Hendra F, F-HA, or F-Myc, along with Hendra G. Surprisingly, when cell−cell fusion was analyzed 48 h post-transfection, Hendra F-HA significantly stimulated syncytia formation, while Hendra F-Myc had fusion levels comparable with the level of wild-type F (Figure 3A). Syncytia formation was also examined at 32 °C, as lower levels of fusion are expected for the wild-type, while hyperfusogenic mutants can overcome the energetic barrier and efficiently promote fusion at lower temperatures (*32*, *33*). Eighteen hours post-transfection, the cells were cooled to 32 °C, and syncytia formation was analyzed 72 h later (Figure 3B). Syncytia formation promoted by Hendra F-Myc was similar to that of the wild-type, while Hendra F-HA significantly increased the level of syncytia formation compared to that of the wild-type (Figure 3B), confirming that this mutant is hyperfusogenic.

The Hendra F-HA and F-Myc levels of fusion were also quantified using a luciferase reporter gene assay. Wild-type or tagged Hendra F along with Hendra G and a plasmid containing the luciferase gene under the control of T7 promoter were transfected in Vero cells. Twenty-four hours later, Vero cells were overlaid with BSR cells, which stably express T7 polymerase (*34*). Thus, fusion between the two cell populations leads to luciferase production. In agreement with the syncytia assay data, Hendra F-HA displayed fusion levels that were approximately 200% of that of wild-type F, while Hendra F-Myc had fusion levels comparable with that of wild-type F, indicating that the sequence of the HA tag specifically stimulates membrane fusion when added to the C-terminus of the Hendra F protein (Figure 3C). Work from our laboratory recently compared Hendra F surface expression and fusion activity and found that increased surface densities resulted in increased levels of fusion (*35*). This correlation was not completely linear, with surface densities of 60−75% of that of the wild-type, as seen for F-Myc, corresponding to fusion levels of 80−95% of that of the wild-type, suggesting that Hendra F-Myc displays a normal fusogenic phenotype (*35*).

Previous work by Plemper et al. (*36*) showed that addition of an HA tag to the measles virus (Edmonston strain) attachment protein led to increased fusogenicity of recombinant measles virus, and this was correlated with a decrease in the extent of F−H interaction (*36*). To investigate if the HA tag also stimulates fusion when it is added to the cytoplasmic tail of Hendra G, we performed the fusion assays in the presence of Hendra G-HA.

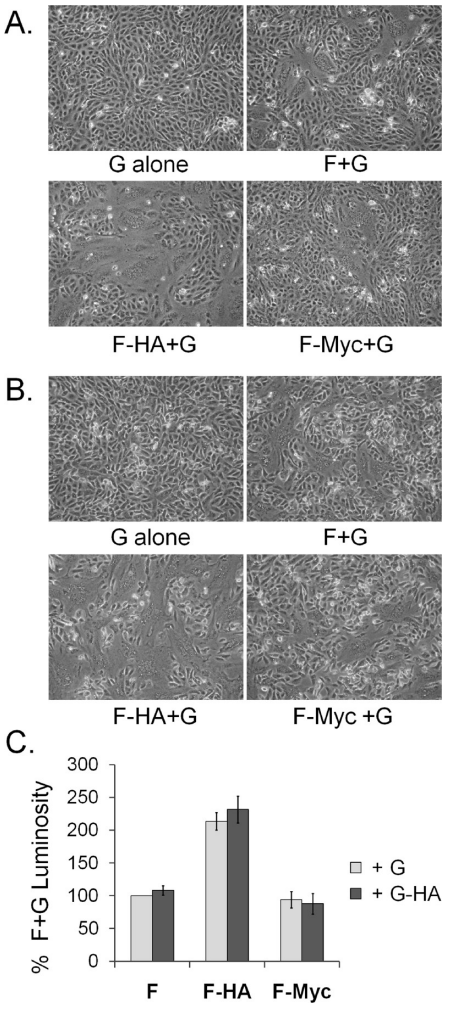


FIGURE 3: Fusion activity of Hendra F, F-HA, F-Myc. (A) Syncytia formation at 37 °C. Hendra F, F-HA, and F-Myc were expressed in Vero cells together with the Hendra G attachment protein, using the pCAGGS expression system. Forty-eight hours post-transfection, cells were photographed at 100× magnification and examined for syncytia formation. (B) Syncytia formation at 32 °C. The proteins were expressed as described above, and 18 h post-transfection, the cells were transferred to 32 °C. Seventy-two hours post-transfection, the cells were photographed as described above. (C) Luciferase assay for cell−cell fusion. Wild-type or tagged Hendra glycoproteins and T7 luciferase reporter gene plasmids were transfected into Vero cells, at a 1:2 F:G ratio. Twenty hours post-transfection, Vero cells were overlaid with T7 polymerase-expressing BSR cells and incubated for 3 h at 37 °C. Cells were lysed, and luciferase activity was measured on a luminometer. The fusion activity was examined both in the presence of wild-type G (+G) and in the presence of HA-tagged Hendra G (+G-HA). Numbers are normalized as percentages of the luminosity of wild-type F and G. The graph represents results from six independent experiments, and the error bars represent the 95% confidence interval.

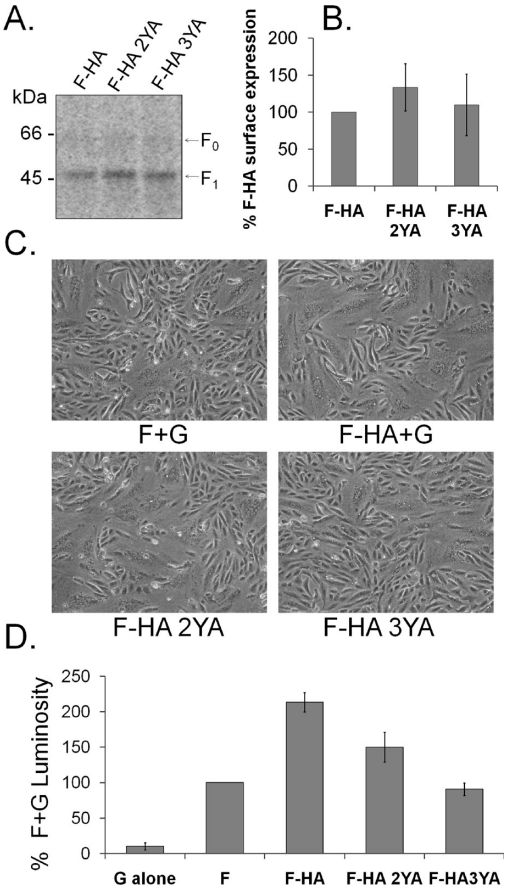


FIGURE 4: Surface expression and fusion activity of Hendra F-HA, F-HA2YA, and F-HA3YA. (A) Surface expression. Vero cells expressing wild-type F or the tagged glycoproteins were metabolically labeled for 15 h, followed by biotinylation of the surface proteins. Proteins were immunoprecipitated, and the surface population was separated using streptavidin agarose beads. Proteins were resolved on a 15% SDS−PAGE gel and visualized using the Typhoon imaging system. (B) Quantitation of Hendra F-HA, F-HA2YA, and F-HA3YA. Results represent the average of three independent experiments, and the error bars represent the 95% confidence interval. (C) Syncytia formation. Hendra F, F-HA, F-HA2YA, and F-HA3YA were expressed in Vero cells along with the Hendra G attachment protein. Forty-eight hours post-transfection, cells were photographed at 100× magnification and examined for syncytia formation. (D) Luciferase reporter gene assay. Wild-type or tagged Hendra glycoproteins and T7 luciferase reporter gene plasmids were transfected into Vero cells, with a 1:2 F:G ratio. Twenty hours post-transfection, Vero cells were overlaid with T7 polymerase-expressing BSR cells and incubated for 3 h at 37 °C. Luciferase activity was measured on a luminometer, and the data were normalized as percentages of the luminosity of wild-type F and G. The graph represents results from five independent experiments, and the error bars represent the 95% confidence interval.

However, no significant changes in the levels of fusion were observed (Figure 3C), suggesting that the HA tag specifically alters measles virus attachment protein but not Hendra G protein, indicating that mechanistic differences between the two systems are present.

*The Three Tyrosine Residues Present in the HA Tag Modulate Membrane Fusion*. Comparison of the sequences of the HA (YPYDVPDYA) and Myc (EQKLISEEDL) tags shows that the HA tag is more hydrophobic and also contains three tyrosine residues, while the Myc tag contains a large number of charged, polar amino acids, with no aromatic residues. Recent data from our laboratory showed that cytoplasmic tail aromatic residues modulate Hendra F protein-promoted membrane fusion (Gibson et al., manuscript in preparation). To test the potential role of the HA tag tyrosine residues, we created two additional mutants, F-HA2YA, in which the first two tyrosine residues in the HA tag were substituted with alanine, and F-HA3YA, in which all three tyrosine residues were mutated to alanine (Figure 1).

Surface expression of Hendra F-HA2YA and 3YA was analyzed by biotinylation following an overnight label (Figure 4A), and their surface densities were found to be slightly higher than that of Hendra F-HA (Figure 4B). The fusion activity of the

mutants was examined by syncytia assays (Figure 4C) and reporter gene assays (Figure 4D), as described above. Hendra F-HA2YA formed syncytia at levels slightly lower than that of Hendra F-HA, while Hendra F-HA3YA formed syncytia at levels lower than that of F-HA and had fusion levels comparable with that of the wild-type protein (Figure 4C). When quantified by the reporter gene assay, the level of membrane fusion promoted by F-HA2YA was ~25% lower than that of F-HA. The extent of F-HA3YA fusion was approximately half of that observed for F-HA and comparable to that of wild-type Hendra F (Figure 4D). These results demonstrate that the hyperfusogenic phenotype observed for Hendra F-HA is directly related to the presence of three C-terminal tyrosine residues and implicate aromatic residues in the C-terminus of the protein in modulation of Hendra F protein-promoted membrane fusion.

The Nipah virus fusion protein was reported to associate with lipid raft domains, but the majority of Nipah F was found in nonraft fractions (80%) (*20*). However, Nipah F hypofusogenic mutants were found to associate with lipid domains at similar or lower percents than the wild-type protein, suggesting that the association with the lipid domains is not a determining factor of Nipah F fusogenicity (*20*). To test if the CT tyrosine residues alter the association of Hendra F with the lipid domains, we examined Hendra F insolubility after Triton X-100 extraction. Similar to the Nipah F study (*20*), approximately 20% of Hendra F was associated with lipid microdomains, and no differences in lipid raft association were observed among wild-type Hendra F, F-HA, F-HA2YA, and F-HA3YA (data not shown).

*The HA Tag Does Not Stimulate PIV5 F Fusion Activity*. The dramatic fusion stimulation observed with Hendra F-HA was unexpected. To check if the addition of the HA tag to the cytoplasmic tail stimulated fusion promoted by other paramyxovirus fusion proteins, the HA epitope tag was added to the cytoplasmic tail of the distantly related PIV5 fusion protein or the closely related Nipah virus fusion protein. For PIV5 F, the protein surface expression and cleavage state were analyzed by surface biotinylation after an overnight label (Figure 5A). Although PIV5 F-HA was expressed and proteolytically cleaved, the surface density for this mutant was approximately 35% of that of PIV5 F, suggesting that the HA tag alters PIV5 F protein expression or stability. The fusion activity of PIV F-HA was tested using the syncytia assay and the reporter gene assay, as described above. The syncytia assay showed a decrease in the level of fusion mediated by PIV5 F-HA relative to PIV5 F (Figure 5C). The luciferase reporter gene assay indicated that the level of fusion promoted by PIV5 F-HA was approximately 25% of that of wild-type PIV5 F (Figure 5B), whereas its level of surface expression was ~35% of that of PIV5 F. These results suggest that the HA tag does not have a significant stimulatory effect on fusion promoted by PIV5 F-HA, as previous studies have shown that PIV5 F surface densities and the fusion activity correlate in an approximately linear fashion (*37*, *38*). In contrast, HA-tagged Nipah F gave an increased level of fusion by both reporter gene and syncytia assays when transfected at levels similar to those of the wild-type Nipah F (data not shown), suggesting that the stimulatory effect of C-terminal tyrosines is conserved among the Henipavirus F proteins.

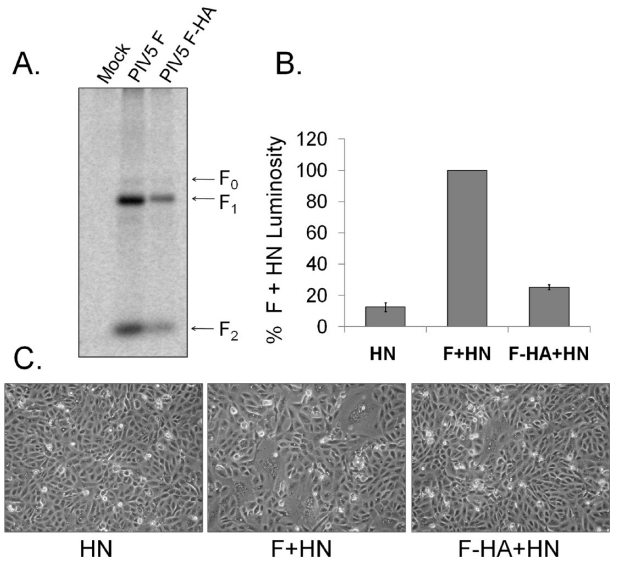


FIGURE 5: Surface expression and fusion activity of PIV5 F and F-HA. (A) Surface expression. Vero cells expressing PIV5 F or F-HA were metabolically labeled overnight, followed by the biotinylation of the surface proteins. Proteins were immunoprecipitated, and the surface population was separated using streptavidin agarose beads. The proteins were resolved on a 15% polyacrylamide gel and visualized using the Typhoon imaging system. (B) Luciferase reporter gene assay. PIV5 F or F-HA constructs, along with PIV5 HN and a T7 luciferase reporter gene plasmid, were transfected into Vero cells, with a 1:2 F:HN ratio. Twenty hours post-transfection, Vero cells were overlaid with T7 polymerase-expressing BSR cells and incubated for 3 h at 37 °C. Luciferase activity was measured on a luminometer, and the data were normalized as percentages of the luminosity of wild-type F and HN. The data represent results from four independent experiments, and the error bars represent the 95% confidence interval. (C) Syncytia formation. PIV5 F or F-HA was expressed in Vero cells along with PIV5 HN. Forty-eight to seventy-two hours post-transfection, cells were photographed at 100× magnification and examined for syncytia formation.

## DISCUSSION

Our data show that elongating the CT of Hendra F with a small HA epitope tag increases fusion promoted by Hendra F, implicating the C-terminal end of the CT in modulation of Hendra F-promoted membrane fusion. The increase in the level of fusion is not due to the extended length of the CT but to the specific sequence of the HA tag, as elongating the Hendra F CT with a Myc peptide tag of a similar length did not alter the fusion activity of Hendra F. Our findings strongly suggest that three tyrosine residues present in the HA tag are responsible for the stimulation of membrane fusion seen with Hendra F-HA.

The surface density of Hendra F-HA was similar to that of wild-type Hendra F, indicating that the increase in the level of fusion seen for F-HA was not due to changes in surface expression (Figure 2B). In addition, the surface density of Hendra F-HA was similar to that of wild-type F when it was expressed alone or together with Hendra G (Figure 2D), suggesting that the attachment protein does not alter Hendra F-HA surface expression. Hendra F-HA was proteolytically processed at similar rates with wild-type F, indicating that the hyperfusogenic phenotype was not due to alterations in its cleavage state.

Previous work has shown that changes in the CT of some class I viral fusion proteins can inhibit membrane fusion and alter the formation of the six-helix bundle (*39*−*41*), but it remains unclear how and at what step the CT interferes with the fusion process. Truncations of the CT of NDV, PIV3, and PIV5 greatly decrease the level of or abolish membrane fusion (*42*−*44*). Deletion of the CT of PIV5 was shown to inhibit fusion pore expansion (*45*), while deletion of the CT of HPIV3 strongly affects F oligomerization (*44*). However, removal of the CT did not affect fusion

activity for HPIV2 (*44*). In addition to the CT truncations, it has also been shown that increasing the length of the CT can also inhibit membrane fusion. Elongation of the CT of influenza virus hemagglutinin with one to six histidine residues significantly reduced fusion activity (*46*). Moreover, some retroviral fusion proteins with longer CTs (e.g., Moloney murine leukemia virus and Mason-Pfizer monkey virus) have to be partially cleaved by a viral protease to efficiently promote fusion (*47*−*50*), and truncations in the CT of HIV Env have been shown to increase the level of syncytia formation (*51*) . The CT of the fusion protein of SER virus, the porcine variant of PIV5, is 22 amino acids longer than that of PIV5 F, but SER F is unable to promote syncytia formation (*41*). However, recent studies have shown that it is not the length of the SER F CT per se that alters membrane fusion, but the sequence of the CT (*41*). In the case of SER F, two CT leucine residues are responsible for inhibiting membrane fusion, and their substitution with alanine completely restores fusion to levels similar to that with PIV5 F (*41*). Taken together, these studies demonstrate that the CT can be an important modulator of folding and fusion, but a global understanding of the mechanism remains to be elucidated.

It is possible that the HA tag tyrosine residues alter protein−protein interactions within the F trimer, leading to an increase in the level of membrane fusion. Waning and colleagues have shown that elongating the CT of PIV5 F protein with elements that stabilize the F trimer prevents the ectodomain conformational changes needed for fusion activity (*40*), leading to a significant decrease in the level of fusion (*40*). As Hendra F-HA displays a hyperfusogenic phenotype, destabilization of protein−protein interactions by the HA tag is possible, but a mechanism for this is not clear. It is also possible that the tyrosine residues are involved in interactions with other cellular proteins. Weise and colleagues have recently shown that the tyrosine residues within Nipah fusion and attachment protein cytoplasmic tails are important for proper basolateral trafficking in polarized epithelial cells, and interaction with cytosolic adaptor proteins has been discussed (*52*). While our studies were not conducted in polarized cells, interaction of C-tail tyrosines with specific cellular proteins could well alter the promotion of membrane fusion.

Alternatively, the CT residues may influence association with the plasma membrane. Once fusion is triggered, the HRB regions separate, and major conformational changes lead to the formation of a six-helix bundle, where HRB and HRA are positioned in an antiparallel arrangement (*2*) . During the fusion process, the TM domains must rotate in the plane of the membrane, with the C-terminal region of the TM going deeper into the bilayer, potentially pulling at least part of the CT into the lipid interface and rearranging the lipid phase (*26*, *53*). Interestingly, the CT of several class I fusion proteins (HIV-1 Env, severe acute respiratory syndrome coronavirus S, and influenza virus HA) has been suggested to associate with the plasma membrane, potentially dehydrating the viral membranes and minimizing the energy required for pore enlargement (*2*, *39*, *54*, *55*). For coronavirus S, it was shown that decreasing the level of palmitoylation of the juxtamembranous cysteine residues leads to a reduction in the level of membrane fusion and viral entry (*39*). Statistical evidence from analysis of proteins of known structure has shown that aromatic residues are highly enriched at the membrane−water interface and have a strong tendency to partition into this interface (*56*, *57*). Furthermore, in monotopic proteins, which associate with the surface of membranes but lack a TM domain, it was shown that a high percentage of Tyr and Trp residues are directed toward the membrane, playing roles in stabilizing and anchoring the proteins (*57*). It is possible that the tyrosine residues in the HA tag associate with the plasma membrane at the membrane−water interface, causing the Hendra F CT to loop back toward the lipid bilayer. This could potentially destabilize and/or dehydrate the lipid phase, minimizing the energy required for membrane fusion, as proposed previously (*2*, *26*). This would facilitate the rotation of the TM within the bilayer, correlating with the increased levels of fusion.

Interestingly, a recent study (*58*) showed that the $\sigma$2 subunit of adaptor protein (AP) 2 can bind to the Myc tag because of its resemblance to the acidic dileucine [ED]xxxl[LI] endocytosis motif. Moreover, the structure of AP2 in which both YxxΦ and [ED]xxxl[LI] binding sites are occupied suggests that a molecule containing both these motifs could use both of them to interact with AP2 only if the two endocytosis motifs are at least 25 residues apart. However, the Hendra F YSRL and Myc EQKLI motifs are only 18 residues apart, suggesting that only one of these motifs at a time can be used for AP2 binding and the Hendra F endocytosis needed for subsequent cathepsin L proteolytic processing. Thus, the Myc acidic dileucine-like motif may interfere with binding of Hendra F CT YSRL to AP2, leading to the slowed cathepsin L processing seen for Hendra F-Myc.

The HA tag did not increase the level of fusion when added to the CT of PIV5 F, implying that the length of CT and/or other tail residues contribute to the fusogenic phenotype seen with Hendra F. PIV5 has a shorter 19-amino acid CT, and in contrast to the Hendra F CT, it contains a stretch of seven hydrophobic amino acids next to the TM domain, which could contribute to the interaction of PIV5 F CT with the lipid bilayer. In addition, the PIV F CT also contains two aromatic amino acids toward its C-terminus (FVY) and a basic lysine at the C-terminus, which could participate in interactions with the negative charge of the lipid headgroup.

Taken together, these results demonstrate that the addition of short peptide tags to the CT of paramyxovirus F proteins can significantly and specifically alter fusion activity and proteolytic processing within the endocytic pathway, confirming the importance of this region for protein function and indicating that careful examination of these functions should be performed before using the tagged proteins for further studies.

## ACKNOWLEDGMENT

We are grateful to Lin-Fa Wang of the Australian Animal Health Laboratory for the Hendra virus F and G plasmids and to Robert Lamb (Howard Hughes Medical Institute, Northwestern University) for the pCAGGS-SV5 F expression vector. Karl-Klaus Conzelman (Max Pettenkofer Institut) kindly offered the BSR cells. We also thank the members of the Dutch lab for critical reviews of the manuscript and Dana Ravid (Northwestern University) for assistance with the membrane raft extraction protocol.

## REFERENCES

1. Lamb, R. A., and Kolakofsky, D. (2001) *Paramyxoviridae*: The viruses and their replication. In Fields Virology (Knipe, D. M., and Howley, P. M., Eds.) 4th ed., pp 1305−1340, Lippincott-Raven Press, New York.
2. White, J. M., Delos, S. E., Brecher, M., and Schornberg, K. (2008) Structures and mechanisms of viral membrane fusion proteins: Multiple variations on a common theme. *Crit. Rev. Biochem. Mol. Biol. 43*, 189–219.
3. Eaton, B. T., Broder, C. C., Middleton, D., and Wang, L. F. (2006) Hendra and Nipah viruses: Different and dangerous. *Nat. Rev. Microbiol. 4*, 23–35.

4. Carter, J. R., Pager, C. T., Fowler, S. D., and Dutch, R. E. (2005) The role of N-linked glycosylation of the Hendra virus fusion protein. *J. Virol. 79*, 7922–7925.
5. Bolt, G., and Pedersen, I. R. (1998) The role of subtilisin-like proprotein convertases for cleavage of the measles virus fusion glycoprotein in different cell types. *Virology 252*, 387–398.
6. Ortmann, D., Ohuchi, M., Angliker, H., Shaw, E., Garten, W., and Klenk, H.-D. (1994) Proteolytic cleavage of wild type and mutants of the F protein of human parainfluenza virus type 3 by two subtilisin-like endoproteases, furin and KEX2. *J. Virol. 68*, 2772–2776.
7. Garten, W., Hallenberger, S., Ortmann, D., Schafer, W., Vey, M., Angliker, H., Shaw, E., and Klenk, H. D. (1994) Processing of viral glycoproteins by the subtilisin-like endoprotease furin and its inhibition by specific peptidylchloroalkylketones. *Biochimie 76*, 217–225.
8. Zimmer, G., Budz, L., and Herrler, G. (2001) Proteolytic activation of respiratory syncytial virus fusion protein. Cleavage at two furin consensus sequences. *J. Biol. Chem. 276*, 31642–31650.
9. Meulendyke, K. A., Wurth, M. A., McCann, R. O., and Dutch, R. E. (2005) Endocytosis plays a critical role in proteolytic processing of the Hendra virus fusion protein. *J. Virol. 79*, 12643–12649.
10. Pager, C. T., and Dutch, R. E. (2005) Cathepsin L is involved in proteolytic processing of the Hendra virus fusion protein. *J. Virol. 79*, 12714–12720.
11. Pager, C. T., Craft, W. W., Jr., Patch, J., and Dutch, R. E. (2006) A mature and fusogenic form of the Nipah virus fusion protein requires proteolytic processing by cathepsin L. *Virology 346*, 251–257.
12. Diederich, S., Moll, M., Klenk, H. D., and Maisner, A. (2005) The Nipah virus fusion protein is cleaved within the endosomal compartment. *J. Biol. Chem. 280*, 29899–29903.
13. Vogt, C., Eickmann, M., Diederich, S., Moll, M., and Maisner, A. (2005) Endocytosis of the Nipah virus glycoproteins. *J. Virol. 79*, 3865–3872.
14. Whitman, S. D., Smith, E. C., and Dutch, R. E. (2009) Differential rates of protein folding and cellular trafficking for the Hendra virus F and G proteins: Implications for F-G complex formation. *J. Virol. 83*, 8998–9001.
15. Smith, E. C., Popa, A., Chang, A., Masante, C., and Dutch, R. E. (2009) Viral entry mechanisms: The increasing diversity of paramyxovirus entry. *FEBS J. 276*, 7217–7227.
16. Negrete, O. A., Levroney, E. L., Aguilar, H. C., Bertolotti-Ciarlet, A., Nazarian, R., Tajyar, S., and Lee, B. (2005) EphrinB2 is the entry receptor for Nipah virus, an emergent deadly paramyxovirus. *Nature 436*, 401–405.
17. Bonaparte, M. I., Dimitrov, A. S., Bossart, K. N., Crameri, G., Mungall, B. A., Bishop, K. A., Choudhry, V., Dimitrov, D. S., Wang, L. F., Eaton, B. T., and Broder, C. C. (2005) Ephrin-B2 ligand is a functional receptor for Hendra virus and Nipah virus. *Proc. Natl. Acad. Sci. U.S.A. 102*, 10652–10657.
18. Bishop, K. A., Hickey, A. C., Khetawat, D., Patch, J. R., Bossart, K. N., Zhu, Z., Wang, L. F., Dimitrov, D. S., and Broder, C. C. (2008) Residues in the stalk domain of the hendra virus g glycoprotein modulate conformational changes associated with receptor binding. *J. Virol. 82*, 11398–11409.
19. Bishop, K. A., Stantchev, T. S., Hickey, A. C., Khetawat, D., Bossart, K. N., Krasnoperov, V., Gill, P., Feng, Y. R., Wang, L., Eaton, B. T., Wang, L. F., and Broder, C. C. (2007) Identification of hendra virus g glycoprotein residues that are critical for receptor binding. *J. Virol. 81*, 5893–5901.
20. Aguilar, H. C., Matreyek, K. A., Choi, D. Y., Filone, C. M., Young, S., and Lee, B. (2007) Polybasic KKR motif in the cytoplasmic tail of Nipah virus fusion protein modulates membrane fusion by inside-out signaling. *J. Virol. 81*, 4520–4532.
21. Baker, K. A., Dutch, R. E., Lamb, R. A., and Jardetzky, T. S. (1999) Structural basis for paramyxovirus-mediated membrane fusion. *Mol. Cell 3*, 309–319.
22. Yin, H. S., Wen, X., Paterson, R. G., Lamb, R. A., and Jardetzky, T. S. (2006) Structure of the parainfluenza virus 5 F protein in its metastable, prefusion conformation. *Nature 439*, 38–44.
23. Chen, L., Gorman, J. J., McKimm-Breschkin, J., Lawrence, L. J., Tulloch, P. A., Smith, B. J., Colman, P. M., and Lawrence, M. C. (2001) The structure of the fusion glycoprotein of Newcastle disease virus suggests a novel paradigm for the molecular mechanism of membrane fusion. *Structure 9*, 255–266.
24. Colman, P. M., and Lawrence, M. C. (2003) The structural biology of type I viral membrane fusion. *Nat. Rev. Mol. Cell Biol. 4*, 309–319.
25. Yin, H. S., Paterson, R. G., Wen, X., Lamb, R. A., and Jardetzky, T. S. (2005) Structure of the uncleaved ectodomain of the paramyxovirus (hPIV3) fusion protein. *Proc. Natl. Acad. Sci. U.S.A. 102*, 9288–9293.
26. Schroth-Diez, B., Ludwig, K., Baljinnyam, B., Kozerski, C., Huang, Q., and Herrmann, A. (2000) The role of the transmembrane and of the intraviral domain of glycoproteins in membrane fusion of enveloped viruses. *Biosci. Rep. 20*, 571–595.
27. Langosch, D., Hofmann, M., and Ungermann, C. (2007) The role of transmembrane domains in membrane fusion. *Cell. Mol. Life Sci. 64*, 850–864.
28. Pager, C. T., Wurth, M. A., and Dutch, R. E. (2004) Subcellular localization and calcium and pH requirements for proteolytic processing of the Hendra virus fusion protein. *J. Virol. 78*, 9154–9163.
29. Gardner, A. E., and Dutch, R. E. (2007) A conserved region in the $F_2$ subunit of paramyxovirus fusion proteins is involved in fusion regulation. *J. Virol. 81*, 8303–8314.
30. Whitman, S. D., and Dutch, R. E. (2007) Surface density of the Hendra G protein modulates Hendra F protein-promoted membrane fusion: Role for Hendra G protein trafficking and degradation. *Virology 363*, 419–429.
31. Niwa, H., Yamamura, K., and Miyazaki, J. (1991) Efficient selection for high-expression transfectants by a novel eukaryotic vector. *Gene 108*, 193–200.
32. West, D. S., Sheehan, M. S., Segeleon, P. K., and Dutch, R. E. (2005) Role of the simian virus 5 fusion protein N-terminal coiled-coil domain in folding and promotion of membrane fusion. *J. Virol. 79*, 1543–1551.
33. Paterson, R. G., Russell, C. J., and Lamb, R. A. (2000) Fusion protein of the paramyxovirus SV5: Destabilizing and stabilizing mutants of fusion activation. *Virology 270*, 17–30.
34. Buchholz, U. J., Finke, S., and Conzelmann, K. K. (1999) Generation of bovine respiratory syncytial virus (BRSV) from cDNA: BRSV NS2 is not essential for virus replication in tissue culture, and the human RSV leader region acts as a functional BRSV genome promoter. *J. Virol. 73*, 251–259.
35. Smith, E. C., and Dutch, R. E. (2010) Side chain packing below the fusion peptide strongly modulates triggering of the Hendra virus F protein. *J. Virol. 84*, 10928–10932.
36. Plemper, R. K., Hammond, A. L., Gerlier, D., Fielding, A. K., and Cattaneo, R. (2002) Strength of envelope protein interaction modulates cytopathicity of measles virus. *J. Virol. 76*, 5051–5061.
37. Dutch, R. E., Joshi, S. B., and Lamb, R. A. (1998) Membrane fusion promoted by increasing surface densities of the paramyxovirus F and HN proteins: Comparison of fusion reactions mediated by simian virus 5 F, human parainfluenza virus type 3 F, and influenza virus HA. *J. Virol. 72*, 7745–7753.
38. Russell, C. J., Kantor, K. L., Jardetzky, T. S., and Lamb, R. A. (2003) A dual-functional paramyxovirus F protein regulatory switch segment: Activation and membrane fusion. *J. Cell Biol. 163*, 363–374.
39. Shulla, A., and Gallagher, T. (2009) Role of spike protein endodomains in regulating coronavirus entry. *J. Biol. Chem. 284*, 32725–32734.
40. Waning, D. L., Russell, C. J., Jardetzky, T. S., and Lamb, R. A. (2004) Activation of a paramyxovirus fusion protein is modulated by inside-out signaling from the cytoplasmic tail. *Proc. Natl. Acad. Sci. U.S.A. 101*, 9217–9222.
41. Seth, S., Vincent, A., and Compans, R. W. (2003) Mutations in the cytoplasmic domain of a paramyxovirus fusion glycoprotein rescue syncytium formation and eliminate the hemagglutinin-neuraminidase protein requirement for membrane fusion. *J. Virol. 77*, 167–178.
42. Sergel, T., and Morrison, T. G. (1995) Mutations in the cytoplasmic domain of the fusion glycoprotein of Newcastle disease virus depress syncytia formation. *Virology 210*, 264–272.
43. Bagai, S., and Lamb, R. A. (1996) Truncation of the COOH-terminal region of the paramyxovirus SV5 fusion protein leads to hemifusion but not complete fusion. *J. Cell Biol. 135*, 73–84.
44. Yao, Q., and Compans, R. W. (1995) Differences in the role of the cytoplasmic domain of human parainfluenza virus fusion proteins. *J. Virol. 69*, 7045–7053.
45. Dutch, R. E., and Lamb, R. A. (2001) Deletion of the cytoplasmic tail of the fusion (F) protein of the paramyxovirus simian virus 5 (SV5) affects fusion pore enlargement. *J. Virol. 75*, 5363–5369.
46. Ohuchi, M., Fischer, C., Ohuchi, R., Herwig, A., and Klenk, H.-D. (1998) Elongation of the cytoplasmic tail interferes with the fusion activity of influenza virus hemagglutinin. *J. Virol. 72*, 3554–3559.
47. Januszeski, M. M., Cannon, P. M., Chen, D., Rozenberg, Y., and Anderson, W. F. (1997) Functional analysis of the cytoplasmic tail of Moloney murine leukemia virus envelope protein. *J. Virol. 71*, 3613–3619.
48. Rein, A., Mirro, J., Haynes, J. G., Ernst, S. M., and Nagashima, K. (1994) Function of the cytoplasmic domain of a retroviral transmembrane protein: p15E-p2E cleavage activates the membrane fusion capability of the murine leukemia virus Env protein. *J. Virol. 68*, 1773–1781.

49. Brody, B. A., Rhee, S. S., and Hunter, E. (1994) Postassembly cleavage of a retroviral glycoprotein cytoplasmic domain removes a necessary incorporation signal and activates fusion activity. *J. Virol. 68*, 4620–4627.
50. Melikyan, G. B., Markosyan, R. M., Brener, S. A., Rozenberg, Y., and Cohen, F. S. (2000) Role of the cytoplasmic tail of ecotropic moloney murine leukemia virus Env protein in fusion pore formation. *J. Virol. 74*, 447–455.
51. Murakami, T., Ablan, S., Freed, E. O., and Tanaka, Y. (2004) Regulation of human immunodeficiency virus type 1 Env-mediated membrane fusion by viral protease activity. *J. Virol. 78*, 1026–1031.
52. Weise, C., Erbar, S., Lamp, B., Vogt, C., Diederich, S., and Maisner, A. (2010) Tyrosine residues in the cytoplasmic domains affect sorting and fusion activity of the Nipah virus glycoproteins in polarized epithelial cells. *J. Virol. 84*, 7634–7641.
53. Bissonnette, M. L., Donald, J. E., DeGrado, W. F., Jardetzky, T. S., and Lamb, R. A. (2009) Functional analysis of the transmembrane domain in paramyxovirus F protein-mediated membrane fusion. *J. Mol. Biol. 386*, 14–36.
54. Kliger, Y., and Shai, Y. (1997) A leucine zipper-like sequence from the cytoplasmic tail of the HIV-1 envelope glycoprotein binds and perturbs lipid bilayers. *Biochemistry 36*, 5157–5169.
55. Wyss, S., Dimitrov, A. S., Baribaud, F., Edwards, T. G., Blumenthal, R., and Hoxie, J. A. (2005) Regulation of human immunodeficiency virus type 1 envelope glycoprotein fusion by a membrane-interactive domain in the gp41 cytoplasmic tail. *J. Virol. 79*, 12231–12241.
56. Hong, H., Park, S., Jimenez, R. H., Rinehart, D., and Tamm, L. K. (2007) Role of aromatic side chains in the folding and thermodynamic stability of integral membrane proteins. *J. Am. Chem. Soc. 129*, 8320–8327.
57. Granseth, E., von Heijne, G., and Elofsson, A. (2005) A study of the membrane-water interface region of membrane proteins. *J. Mol. Biol. 346*, 377–385.
58. Jackson, L. P., Kelly, B. T., McCoy, A. J., Gaffry, T., James, L. C., Collins, B. M., Honing, S., Evans, P. R., and Owen, D. J. (2010) A large-scale conformational change couples membrane recruitment to cargo binding in the AP2 clathrin adaptor complex. *Cell 141*, 1220–1229.